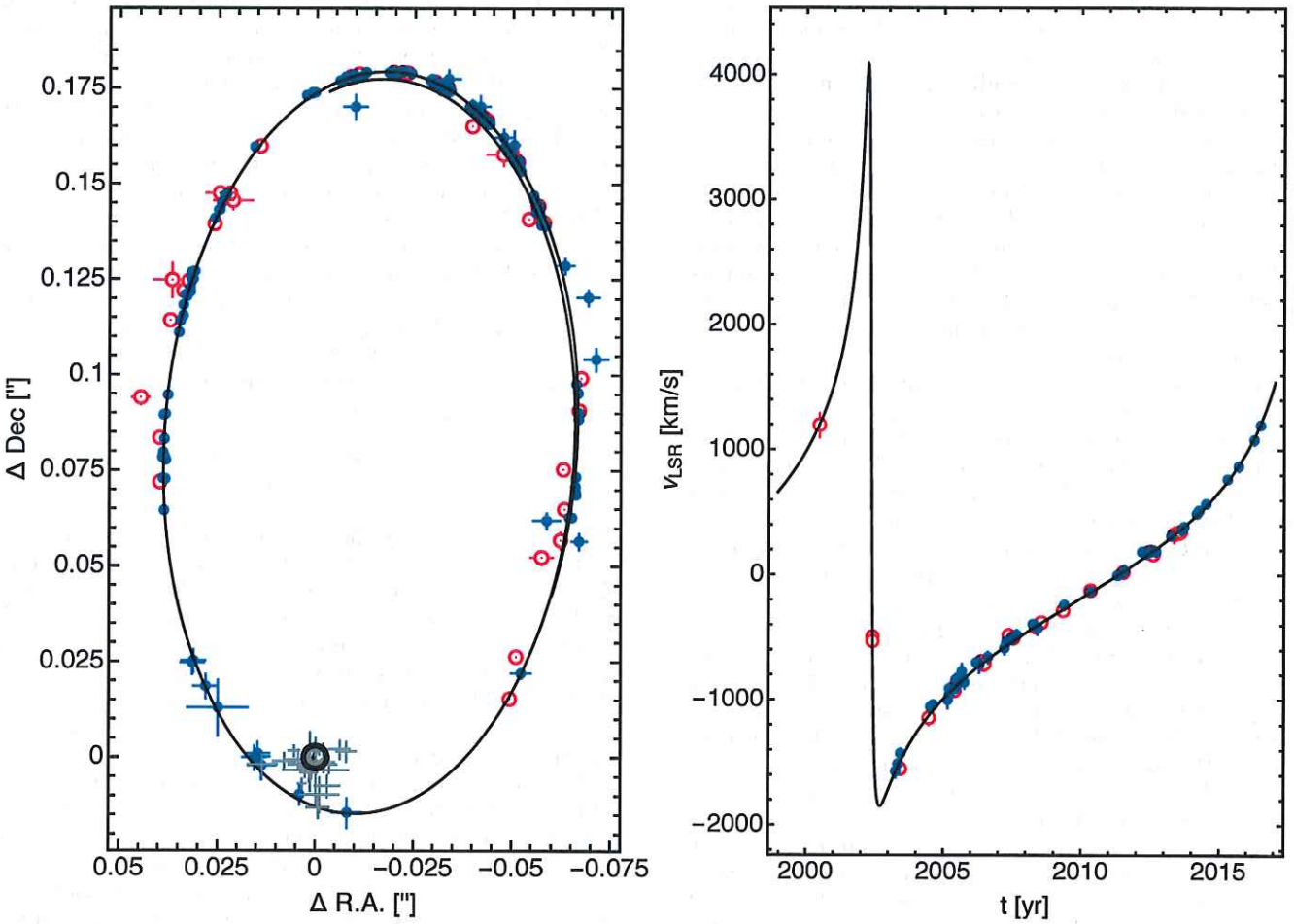

Figure 2. The orbit of the star S2. Left: The measured positions plotted in the plane of sky. The blue data are from the VLT (before 2002: from the NTT), the red data are from Boehle et al. (2016) corrected for the difference in reference coordinate system. The gray data points are positions at which flares have been recorded. The black ellipse is the best fitting orbit, the position of the mass is denoted by the black circle. Note that the fitting procedure matches the functions $\alpha(t)$ and $\delta(t)$, i.e. it does not only match the positions in the plane of sky but rather also in time. The plotted ellipse does not close, since there is a small residual drift motion of the fitted mass in the reference frame. The physical model is purely Keplerian. Right: The measured radial velocities as a function of time. The same best fitting orbit as in the left panel is denoted by the black line.

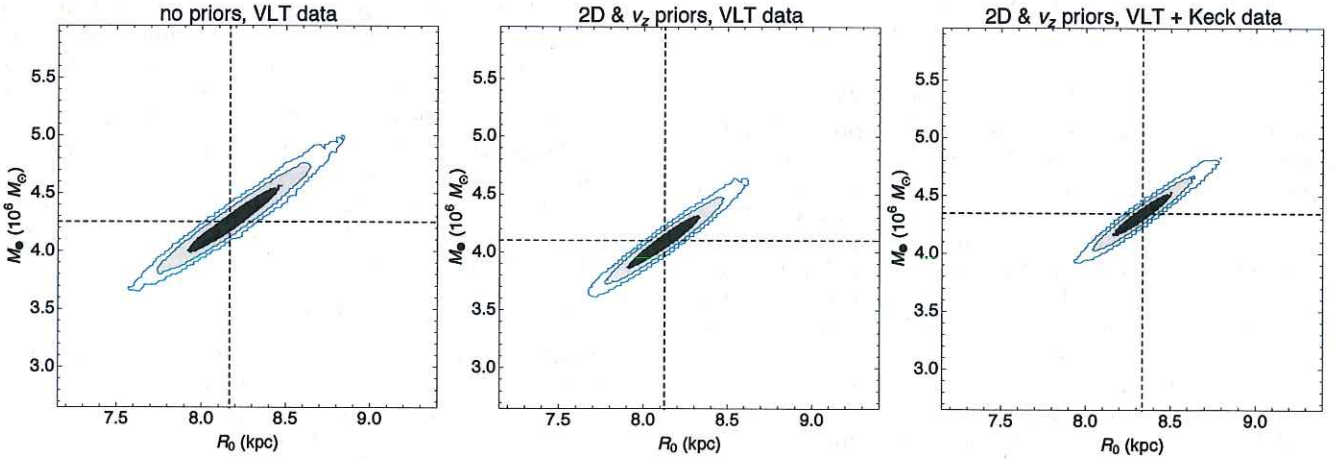

Figure 3. Mass of and distance to Sgr A* from the orbit of S2. The three panels show projections of the respective Markov chains into the mass-distance plane, giving contours at the 1-, 2- and 3-σ level. The dashed lines mark the best fit values. The left panel is for a fit without prior information (row 1 in table 1), the middle panel includes the priors and thus leads to smaller parameter uncertainties (row 2 in table 1). The right panel in addition uses the Keck data from Ghez et al. (2008), which leads to a small shift of the best fitting parameters with virtually unchanged uncertainties (row 3 in table 1).

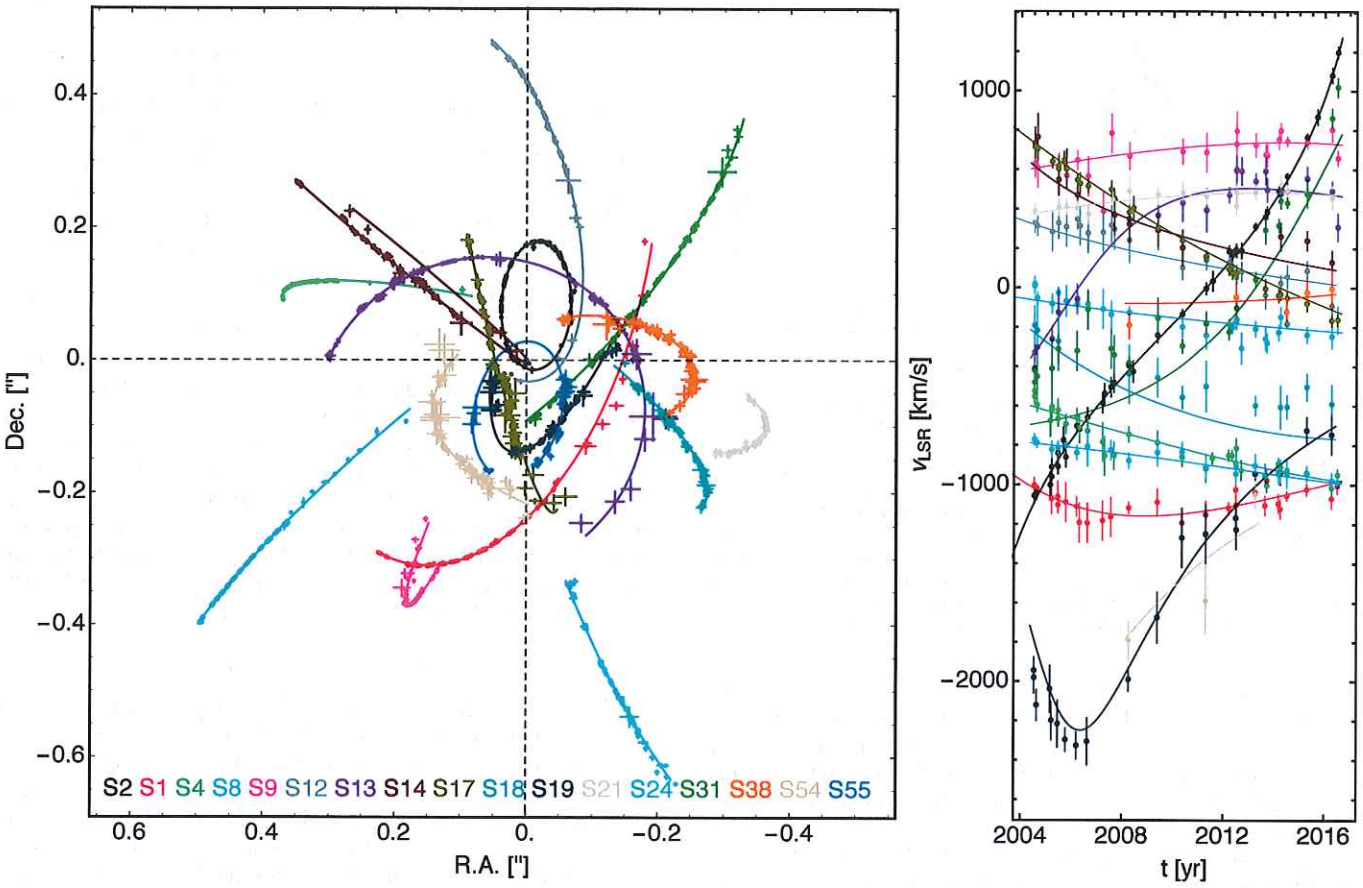

Figure 8. Left: The astrometric data for the 17 stars used for the multi-star fit, shown together with the best-fitting orbits from the multi-star fit (solid lines). The dashed lines mark the position of the mass in this fit. Right: The radial velocity data of the sample, omitting the S2 data before 2004. The color coding is the same as for the left panel. Also, for S55 we don't have any radial velocity information. The solid lines give the best fitting orbits.

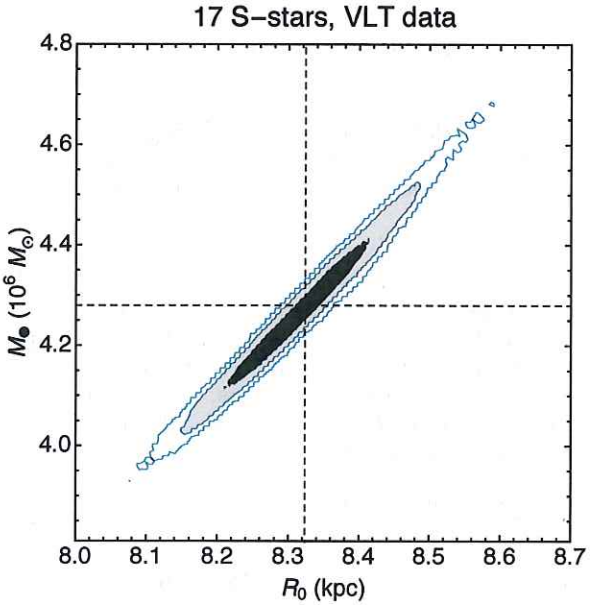

Figure 9. Combined constraint on mass M and distance R_0 using the multi-star fit. Note the different axes scale compared to figures 3 and 4.

the full multi-star fit, so the results are not driven by the S2 data only, and the difference is compatible with our estimate of the systematic error. The best fit value for R_0 in the 16-star fit is at 8.19 kpc, while the mean of the posterior distribution from the Markov chain is at 8.24 kpc, indicative that the best fit value is slightly biased to lower values. This would further reduce the small difference between the 16-star fit and our fiducial 17-star fit.

3.5. *Positions of flares from Sgr A**

An additional cross-check is possible using the flaring emission of Sgr A*. The stellar orbits locate the mass in the infrared coordinate system through orbit fitting. The location of the radio source Sgr A* in the infrared coordinate system is based on the SiO masers (Plewa et al. 2015). The flares from Sgr A* locate the source directly in the infrared coordinate system.

Our data set contains 88 images in which we can identify the variable, radiative counterpart of Sgr A* in the near-infrared. Fitting the positions with a linear motion yields a velocity of $(v_{\mathrm{R.A.}}, v_{\mathrm{Dec.}}) = (-48, -41) \pm (174, 332)\,\mu$as/yr, i.e. consistent with being at rest. The error bar has been rescaled to yield a reduced χ^2 of 1. This level of accuracy is similar to the constraints on how well we can fix Sgr A* in the infrared coordinate system (Plewa et al. 2015). Given the zero motion, we can determine the mean position of the flares. It is $(\Delta\,\mathrm{R.A.}, \Delta\,\mathrm{Dec.}) = (-0.73, 0.77) \pm (0.57, 1.08)$ mas. The errors are dominated by the variance of the individual data points, as one might expect at the most confused